Journal of New Materials for Electrochemical Systems 15, 1-4 (2012)

Electrochemical Performance of Hollow α-Fe_2O_3 Spheres as Anode Material for Lithium-ion Battery

Zhijia Du, Shichao Zhang*, Zhiming Bai, Tao Jiang and Guanrao Liu

School of Materials Science and Engineering, Beihang University, Beijing, 100191, China

Received: July 21, 2011, Accepted: September 1, 2011, Available online: November 14, 2011

Abstract: *Hollow α-Fe_2O_3 spheres were synthesized by a facile hydrothermal method followed by a calcination step. The crystalline structure and morphology of the synthesized materials were characterized by X-ray diffraction (XRD), scanning electron microscopy (SEM) and transmission electron microscopy (TEM). The morphology of the sample consisted of porous hollow spheres that ranged about hundreds of nanometers and were composed of well crystallized nanoparticles about a dozen nm. The electrochemical properties of the sample were evaluated by cyclic voltammetry (CV) and charge/discharge measurements. The discharge/charge capacities in the first cycle achieved 1336/934 mAh g^{-1} at the rate of 0.2 C. The reversible capacity in the 50th cycle remained 840 mAh g^{-1} with impressive retention rate of 90%. This good lithium storage property was probably ascribed to the porous and hollow structure and nanoscale α-Fe_2O_3 particles, which enlarged the surface area and shortened the pathway for lithium ion migration. The appealing electrochemical capability indicated the potential implementation of hollow Fe_2O_3 spheres as anode material for future lithium-ion battery.*

Keywords: α-Fe_2O_3, Nanoparticles, Porous materials, hydrothermal synthesis, lithium-ion batteries

1. INTRODUCTION

The demand for high capacity, long life Li-ion battery has been steadily increasing for future power tools, such as portable electronics and electric/hybrid vehicles [1,2]. Recently, nano-sized 3d-metal oxides MO_x (M= Fe, Co, Ni, etc.) have been extensively researched as anode materials in lithium-ion battery because of their high energy capacity [3,4]. The mechanism of Li react with MO_x involves the formation and decomposition of Li_2O, accompanying the reduction and oxidation of MO_x. The reduction of lithium from Li_2O was thought to be thermodynamically impossible before. However, it was demonstrated to become feasible when the size of MO_x was reduced to nanoscale [4]. Among those transition-metal oxides, iron oxide is considered one of the most appealing anode materials due to its low cost, low environmental impact and abundance of the raw materials. The theoretical capacity of Fe_2O_3 is as high as 1005 mAh g^{-1}, which is much higher than that of the current commercial graphite anode materials (372 mAh g^{-1}). MO_x, including Fe_2O_3, reduction and oxidation with lithium are accompanied by enormous structural change, which induces fast capacity fading and hindrance of practical implementation.

*To whom correspondence should be addressed: Email: csc@buaa.edu.cn
Phone: 86-10-82338148; Fax.: 86-01-82339319

To address this issue, an efficient approach is to design nanostructured Fe_2O_3, such as nanoflowers [5], nanowires [6], nanocapsules [7], nanoflakes [8,9] and nanotubes [10]. These investigations distinctly revealed that the morphology of the nanostructured Fe_2O_3 have great effect upon the lithium storage properties. For instance, hydrothermal method has been carried out to synthesize several α-Fe_2O_3 samples with various morphologies. The electrochemical performance test suggested that the nanospheres presented the highest discharge capacity and impressing cycle performance, which may result from the high surface area as well as small and uniform grain size [11]. Chen's group has prepared porous α-Fe_2O_3 films by electrostatic spray deposition. The α-Fe_2O_3 films displayed both high reversible capacity (1080 mAh g^{-1}) and good cycling performance due to the porous structure which could buffer the volume changes during lithium intercalation/de-intercalation [12]. Therefore, enlargement of the active materials/electrolyte area and decreasing the particle size of the active materials seem to be effective ways to enhance the lithium storage performance.

In this paper, we prepare hollow α-Fe_2O_3 spheres by the facile hydrothermal method and subsequent heat-treatment. The sample shows impressive high capacity and excellent cycling stability, which indicates the potential of their application as electrode mate-

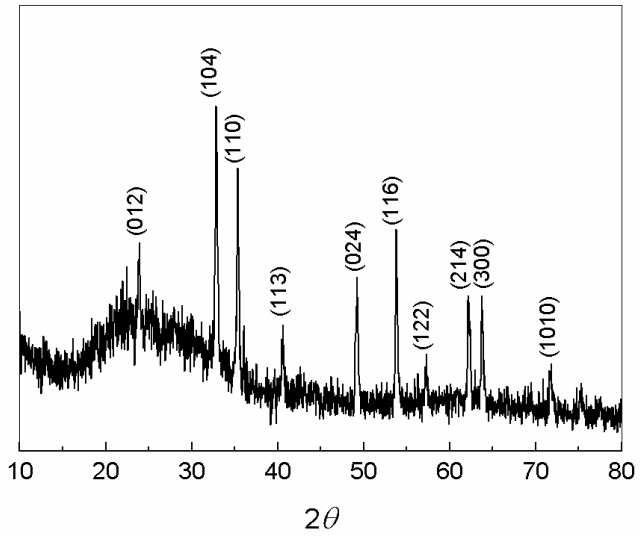

Figure 1. XRD patterns of iron oxide hollow spheres after calcination at 600 °C for 5 h.

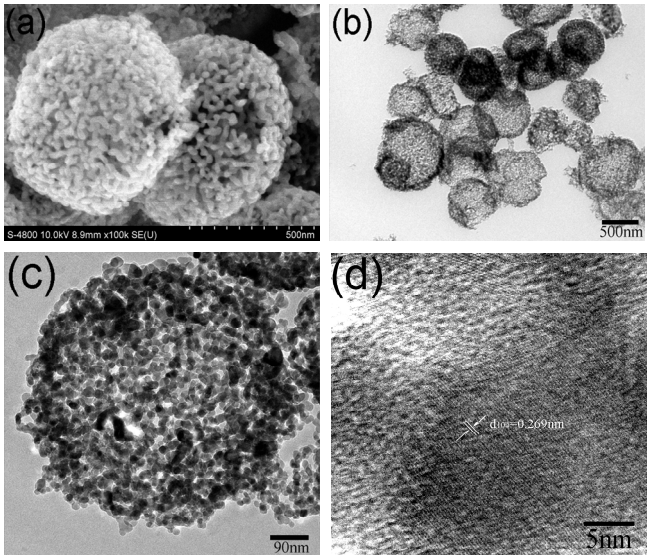

Figure 2. (a) SEM micrograph of the porous hollow Fe_2O_3 spheres, (b) low magnification TEM image of hollow Fe_2O_3 spheres, (c) high magnification TEM image of hollow Fe_2O_3 spheres, and (d) high resolution TEM (HRTEM) image of F_2O_3 nanoparticles.

rials for high performance lithium-ion batteries.

2. EXPERIMENTAL

28 mM Glucose was firstly dissolved in 30 mL deionized water, and then 5.6 mM $(NH_4)_2Fe(SO_4)_2{\cdot}6H_2O$ was dissolved in 15 mL deionzed water. The carbohydrate:metal molar ratio was 5:1 as reported before [13]. The two solutions were mixed and sealed in an autoclave, which was hydrothermal heated at 160 °C for 24 h. The precipitate was then filtered and washed repeatedly with deionized water and ethanol. The products were then calcined at 600 °C for 5 h to form hollow metal oxide partices.

The working electrode was constituted by mixing Fe_2O_3 (active material), polyvinylidene fluoride (binder), and Super P (conducting material) with a weight ratio of 70:10:20. The galvanostatic measurements were carried out at room temperature. Cyclic voltammetry test was performed between 0 and 3 V at a scanning rate of 0.1 mV/s.

The hollow Fe_2O_3 were characterized by a field emission scanning electron microscopy (FE-SEM, Hitachi S-4800) and a field emission transmission electron microscope (FE-TEM, JEM-2100F). Powder X-ray diffraction (XRD) patterns were obtained on a Rigaku D/MAX 2000 PC diffractometer, using Cu Ka radiation (λ=1.5406 Å).

3. RESULTS AND DISCUSSION

Fig. 1 shows the XRD pattern of the final conducts after calcination at 600 °C for 5 h. The diffraction peaks are consistent with the standard hematite (α-Fe_2O_3) rhombohedral structure (JCPDS Card No. 33-0664). The sharp peaks suggest the high crystallinity of the product. Additionally, the broad peak from 15° to 30° is ascribed to the diffraction of the glass substrate which was used to hold the sample.

Fig. 2a shows SEM image of the as-prepared α-Fe_2O_3 products. It clearly certifies that porous hollow Fe_2O_3 spheres consisted of many nanoscale particles were formed after calcinations. In the hydrothermal processing, carbon spheres are formed with metal ion incorporated into their hydrophilic shell while the hollow Fe_2O_3 spheres were obtained after removal of carbon by calcination [13]. Fig. 2b is a low magnification TEM image, showing the hollow sphere structure with diameter about hundreds of nanometers. High magnification TEM image in Fig. 2c distinctly illustrates the individual hollow sphere is actually comprised of many nanoparticles with a size of a dozen nm. Fig. 2d exhibits a HRTEM image of Fe_2O_3 nanoparticles at the shell of the submicron hollow sphere, indicating the sample is well crystallized. The distance between the neighboring lattice planes is 0.270 nm as marked in Fig. 2d. The distance is in agreement with the *d*(104) spacing of rhombohedral α- Fe_2O_3.

Cyclic voltammetry was performed to understand the electrochemical behavior of the sample as shown in Fig. 3a. A substantial difference is clearly exhibited between the first and the subsequent cycles. In the first cathodic process, a sharp peak is recorded at ~0.63 V accompanied by two small peaks at ~0.91 V and ~1.58 V. This is consistent to the mechanism of the first lithium intercalation to α-Fe_2O_3 as reported before [14]. The two small peaks are ascribed to the lithium insertion into the crystal structure of α-Fe_2O_3 and the formation of cubic $Li_2Fe_2O_3$. The sharp peak corresponds to the thorough reduction of iron from Fe^{2+} to Fe^0. Meanwhile, in the anodic process, two broad overlapping peaks were observed at ~1.69 V and ~1.88 V as a consequence of the oxidation of Fe^0 to Fe^{2+} and further oxidation to Fe^{3+} [15]. In the following cycles, both the cathodic and anodic peak potentials shift to ~0.79 V and ~1.73 V, respectively. The cathodic/anodic peak pair is assigned to the reversible oxidation/reduction reaction between α-Fe_2O_3 and Li. It is noticed that the peak current and the integrated area of the peaks are similar. These results reveal the good stability of the

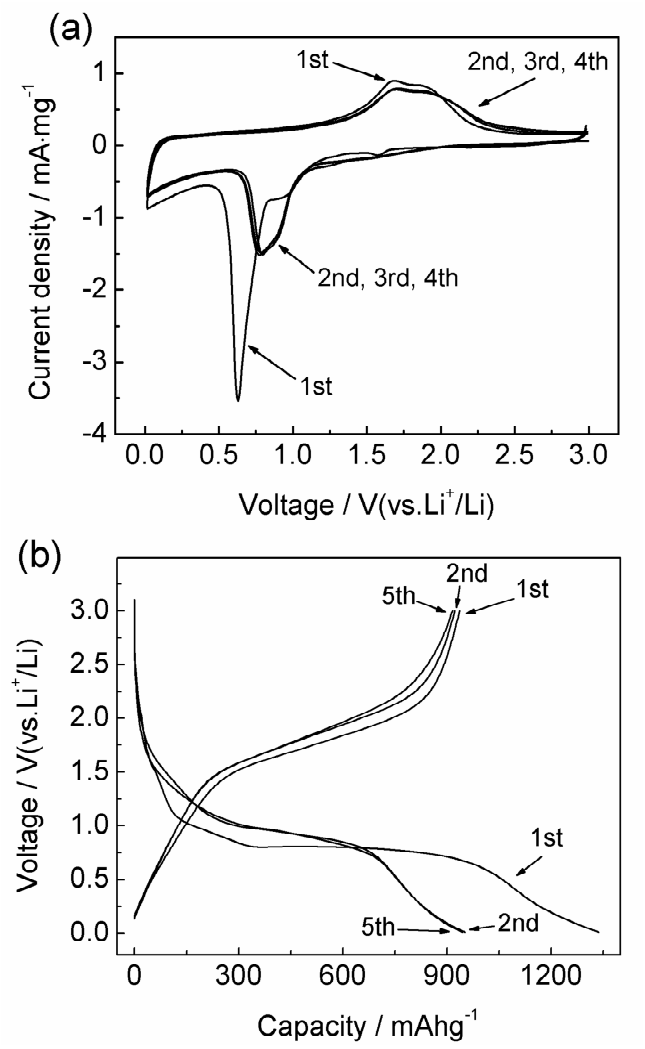

Figure 3. (a) Cyclic voltammetry (CV) curves of the hollow Fe_2O_3 spheres electrode (b) charge/discharge profiles of the hollow Fe_2O_3 spheres electrode with a cut-off voltage of 10 mV–3 V.

lithium intercalation/de-intercalation process in the hollow Fe_2O_3 spheres, due to the hollow structure and nanoscale particles in the shell layer, which shortened the diffusion length of the Li^+ and enhanced the reactivity of iron oxides.

Fig. 3b depicts the voltage profiles of hollow Fe_2O_3 spheres electrodes cycled over a voltage range of 0.01–3 V at 0.2 C rate. In the first discharge curve, the voltage initially drops rapidly to approximately 1.5 V followed by a small slop at 1.5–1.1 V and a wide slop at 1.1–0.8V. The two slops are attributed to the insertion of lithium to α-Fe_2O_3 as discussed in the CV results. The extended plateau at 0.8 V is ascribed to the reduction of Fe^{2+} to Fe^0 [14]. The first discharge capacity is 1336 mAh g^{-1}, which is higher than the theoretical value of Fe_2O_3 (1005 mAh g^{-1}). The excess capacity is probably owing to the formation of a solid electrolyte interphase (SEI) layer because of decomposition of electrolyte on the Fe_2O_3 surface (generally below 0.8 V vs Li^+/Li) [10]. In the following cycles, the lithium intercalation/de-intercalation voltage shifts higher than the

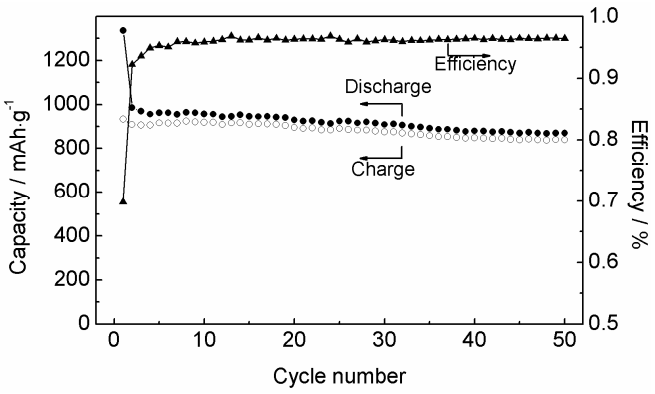

Figure 4. Discharge/charge capacity and Coulombic efficiency versus cycle number for the hollow Fe_2O_3 spheres electrode at 0.2 C rate.

first cycles.

Fig. 4 depicts the charge/discharge (rate = 0.2 C) capacity and Coulombic efficiency versus cycle number plots, providing a direct evidence of the excellent lithium storage performance. Despite the low value of 70% in the first cycle due to the decomposition of electrolyte, the Coulombic efficiency increases quickly in the following cycles (ca. 96% for cycles 7–50). The reversible capacity for the first cycle is 934 mAh g^{-1}, and for the 50th cycle is 840 mAh g^{-1} with retention of 90%. This remarkable enhancement of electrochemical properties can be assigned to the hollow structure and the nanoscale particles in the shell of the sphere. The porous hollow sphere allows complete penetration of the electrolyte, while the nanoscale particles afford short diffusion length of lithium ions and accommodation of volume change during charging/discharging processs.

4. CONCLUSIONS

In summary, hollow spheres with nanoscale α-Fe_2O_3 particles in the porous shell have been successfully synthesized and applied into lithium-ion batteries. Electrochemical measurements of the sample show high capacity and excellent cycle stability. A large capacity of 840 mAh g^{-1} and an appealing capacity retention rate of 90% are accomplished after 50 cycles. This indicates the hollow Fe_2O_3 spheres material is an attractive candidate anode material for future lithium-ion battery.

5. ACKNOWLEDGEMENTS

This work was supported by the National Natural Science Foundation of China (50954005, 51074011), National Basic Research Program of China (2007CB936502), National 863 Program (2006AA03Z230, 2008AA03Z208), the Innovation Foundation of BUAA for PhD Graduates, and the Scholarship Award for Excellent Doctoral Student granted by China Ministry of Education.

REFERENCES

[1] J. B. Goodenough, and Y. Kim, *Chem. Mater.*, 22, 587 (2010).
[2] M. Armand, and J.-M. Tarascon, *Nature*, 451, 652 (2008).

[3] J.-M. Tarascon, and M. Armand, *Nature*, 414, 359 (2001).
[4] P. Poizot, S. Laruelle, S. Grugeon, L. Dupont, J.-M. Tarascon, *Nature*, 407, 496 (2000).
[5] S. Zeng, K. Tang, T. Li, Z. Liang, D. Wang, Y. Wang, Y. Qi, and W. Zhou, *J. Phys. Chem. C*, 112, 4836 (2008).
[6] H. Liu, D. Wexler, and G. Wang, *J. Alloys Compd.*, 487, L24 (2009).
[7] H.S. Kim, Y. Piao, S.H. Kang, T. Hyeon, and Y.E. Sung, *Electrochem. Comm.*, 12, 382 (2010).
[8] L. Chun, X. Wu, X. Lou, and Y. Zhang, *Electrochim. Acta*, 55, 3089 (2010).
[9] M.V. Reddy, T. Yu, C.H. Sow, Z.X. Shen, C.T. Lim, G.V.S. Rao, and B.V.R. Chowdari, *Adv. Func. Mater.*, 17, 2792 (2007).
[10]J. Chen, L. Xu, W. Li, and X. Gou, *Adv. Mater.*, 17, 582 (2005).
[11]Y. NuLi, R. Zeng, P. Zhang, Z. Guo, and H. Liu, *J. Power Sources*, 184, 456 (2008).
[12]L. Wang, H.W. Xu, P.C. Chen, D.W. Zhang, C.X. Ding, and C.H. Chen, *J. Power Sources*, 193, 846 (2009).
[13]M.M. Titirici, M. Antonietti, and A. Thomas, *Chem. Mater.*, 18, 3808 (2006).
[14]D. Larcher, C. Masquelier, D. Bonnin, Y. Chabre, V. Masson, J.B. Leriche, and J.-M. Tarascon. *J. Electrochem. Soc.*, 150, A133 (2003).
[15]J. Morales, L. Sanchez, F. Martin, F. Berry, and X.L. Ren. *J. Electrochem. Soc.*, 152, A1748 (2005).